Egyptian Journal of Petroleum (2014) 23, 247–254

Egyptian Petroleum Research Institute

Egyptian Journal of Petroleum

www.elsevier.com/locate/egyjp
www.sciencedirect.com

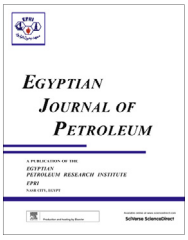

FULL LENGTH ARTICLE

The performance of chemically and physically modified local kaolinite in methanol dehydration to dimethyl ether

Sanaa M. Solyman [a,*], **Mohamed A. Betiha** [b]

[a] *Petrochemical Department, Egyptian Petroleum Research Institute, Nasr City, 11727 Cairo, Egypt*
[b] *Refining Department, Egyptian Petroleum Research Institute, Cairo, Egypt*

Received 21 April 2013; accepted 1 September 2013
Available online 13 October 2014

KEYWORDS

Kaolinite modification;
Characterization;
Dimethyl ether preparation

Abstract The catalytic activity of modified natural kaolinite as a solid acid catalyst for dimethyl ether (DME) preparation was investigated by following up the conversion% of methanol and the yield% of DME. Natural kaolinite (KN) was treated chemically with H_2O_2 (KT) followed by thermal treatment at 500 °C (KC) and then mechano-chemically by ball milling with and without $CaSO_4$ (KB-Ca and KB, respectively). These samples were characterized by XRD, FTIR, SEM, HRTEM, TGA and NH_3-TPD techniques. The different techniques showed that the chemical treatment of kaolinite with H_2O_2 resulted in partial exfoliation/delamination of kaolinite, decreased the amount of acidic sites which is accompanied by increasing their strength. Calcination only decreased the acidic strength and slightly enlarged the particle size mostly due to heat effect. Ball milling resulted in multitude randomly-oriented crystals and increased the amount of acidic sites with the same strength of KT sample. $CaSO_4$ mostly produced ordered monocrystalline kaolinite and created new acidic sites with slightly lower strength relative to KB. The catalytic activity and selectivity depend on the reaction temperature, the space velocity and the strength of acid sites. The most active sample is KB-Ca, which gives 84% DME due to its high amount and strength of acidic sites. The different modification methods resulted in 100% selectivity for DME.

© 2014 Production and hosting by Elsevier B.V. on behalf of Egyptian Petroleum Research Institute.
Open access under CC BY-NC-ND license.

1. Introduction

Dimethyl ether (DME) is of interest in the production of clean fuel, as a chemical intermediate for the preparation of many important chemicals, such as dimethyl sulfate and high-value oxygenated compounds [1–5]. Its physical properties are similar to those of liquefied petroleum gas (LPG), so it is used as a replace or a blend-stock with LPG for home heating and cooking [6,7] and also considered as an alternative for diesel fuel. Recently, the conversion of methanol/DME to triptane (2, 2, 3-trimethylbutane) has spurred particular research interest by Hazari et al. [8]. Practically, triptane is a high-octane and high-value fuel component. DME has been produced by

* Corresponding author. Tel.: +20 2 22747917; fax: +20 2 22747433.
E-mail address: sanaa8763@hotmail.com (S.M. Solyman).
Peer review under responsibility of Egyptian Petroleum Research Institute.

http://dx.doi.org/10.1016/j.ejpe.2014.08.001
1110-0621 © 2014 Production and hosting by Elsevier B.V. on behalf of Egyptian Petroleum Research Institute.
Open access under CC BY-NC-ND license.

catalytic dehydration of methanol over a solid-acid catalyst [6,9–14]. As an alternating process, the direct synthesis of DME from syngas was proposed over bifunctional catalysts, which had two kinds of active sites: one is for methanol formation and the other for methanol dehydration [5,15].

On the other hand, the grinding of kaolinite (either wet or dry) has been the subject of research for a long time which resulted in various effects on the structure and properties often accompanied by structural transformations and chemical reactions [16,17]. Miller and Oulton [18] indicated a prototropy effect on kaolinite during percussive grinding i.e., a transfer of protons from one phase to another that takes place within the structure. Also, Juhasz reviewed the processes involved in grinding kaolinite, and developed tests to study processes during intensive grinding (super grinding), as the mechanical activation of kaolins, including kaolinite and dickite [19]. Also, mechano-chemical activation caused significant changes in the kaolinite structure by increasing the number of lattice defects, surface energy, dehydroxylation temperature and chemical reactivity [19–22].

Modifications of kaolinite surfaces have been studied using a combination of intercalation and thermal treatment [23,24]. New additional phases of kaolinite were found and modification of the hydroxyl surfaces was extensive even with mild heating or due to intense local heating. Schrader observed that the crystal structure was deformed mainly along the *c* axis during mechanical treatment and proved to be more resistant along the *b* axis [25]. The structural changes of kaolinite, especially with respect to its hydroxyl groups (contain outer and inner hydroxyl groups which were designated as OuOH and InOH, respectively), were mainly investigated by means of infrared spectroscopy [21,26].

The request for needed fuels and different chemical feedstocks fluctuates, and as a result, logistical mismatches can occur in furnishing of their raw materials such as coal, biomass, crude oil, and methane. To overcome these challenges, industry requires a versatile, robust suite and economic process of conversion technologies, many of which are mediated by the synthesis of dimethyl ether (DME) as valuable intermediates.

In this paper, natural kaolinite was chemically, thermally, mechanically and mechano-chemically treated and, characterized through XRD, FTIR, HRTEM, SEM, NH_3-TPD and TGA techniques. The catalytic activity of different modified kaolinite samples was investigated in the preparation of DME by methanol dehydration, seriously lacking in the literature as a cheap source for DME. The textural and structural changes in all samples were correlated with conversion% of methanol and selectivity to DME.

2. Experimental

2.1. Kaolinite modification

Firstly, Egyptian natural kaolinite (KN) was treated with hydrogen peroxide (p.a., 30%) to eliminate organic matter. This treatment was conducted by magnetic stirring for 6 h at 60 °C, filtrated off, dried at 110 °C, and denoted as KT. A portion of KT sample is calcined at 500 °C for 8 h, and denoted as KC. A portion of KC sample is ball milled (Planetary Ball Mill PM 400, Tungsten Carbide Balls, 250 rpm) for 8 h with and without 2.5% w/w $CaSO_4$ (denoted as KB-Ca and KB, respectively).

2.2. Characterization

The crystallographic structures of the materials were determined by a powder X-ray diffraction system (XRD, BRUKER axs–D8 ADVANCE) equipped with Cu-Kα radiation (λ = 0.15406 nm).

Fourier transform infrared spectroscopy (FTIR) measurements were performed using Nicolet IS-10 FTIR over the wave number 4000–400 cm^{-1}. High-resolution transmission electron microscopy (HRTEM) image was conducted on a JEOL 2011 (Japan) electron microscope at 200 k V.

Scanning electron microscopy (SEM) images were taken using a JEOL JSM-5300 instrument working at 30 kV.

Temperature programed desorption (NH_3-TPD) of ammonia was measured using a CHEMBET 3000 chemical absorber (Quantachrome). Samples were activated at 500 °C for 1 h in a flow of helium; subsequently ammonia was introduced for 1.5 h at 100 °C. The physically adsorbed ammonia molecules were removed by purging with helium flow until the baseline was flat. The reactor temperature was then increased to 700 °C with a ramping rate of 10 °C/min.

Thermal stability was carried out in a TA Instruments SDTQ 600 simultaneous TGA thermogravimetric analyzer. The analyses were conducted for a total sample mass of 10.0 ± 0.2 mg. The samples were heated under nitrogen flow (100 ml min^{-1}) from 50 to 750 °C, at 20 °C min^{-1}.

2.3. Dehydration method

The vapor phase dehydration of methanol was carried out in a conventional flow type reactor as described in detail in previous work [14]. The reaction temperature ranged from 200 to 500 °C and the catalyst weight is 2.5 g. The reaction products were analyzed on a gas liquid chromatograph (Hewlett Packard-5890) equipped with FID detector and connected with Carbowax backed column.

3. Results and discussion

3.1. Characterization of kaolinite samples

3.1.1. X-ray diffraction analysis

The XRD analysis of (KN), (KT), (KC), (KB) and (KB-Ca) samples indicated the structural formula of $Al_2Si_2O_5(OH)_4$ and is shown in Fig. 1. The XRD pattern of KT shows rapid changes in the kaolinite structure after chemical treatment with H_2O_2. Mostly, H_2O_2 diffused into the interlayer spaces of kaolinite, eliminated the organic contaminants in-between layers, exchanged with water and some alkali earth metal oxides such as MgO and CaO and catalytically decomposed into O_2 and H_2O at 60 °C by Mn oxides located in mineral interlayer. The gas evolved can disrupt individual silicate layers which reflected a slight increase in d-spacing of 0 0 1 plane [27,28]. Also, the relative reflection intensity values (I/I_o) which are simply the ratio between the peak height of modified samples (I) and the corresponding peak in parent kaolinite (I_o) for all

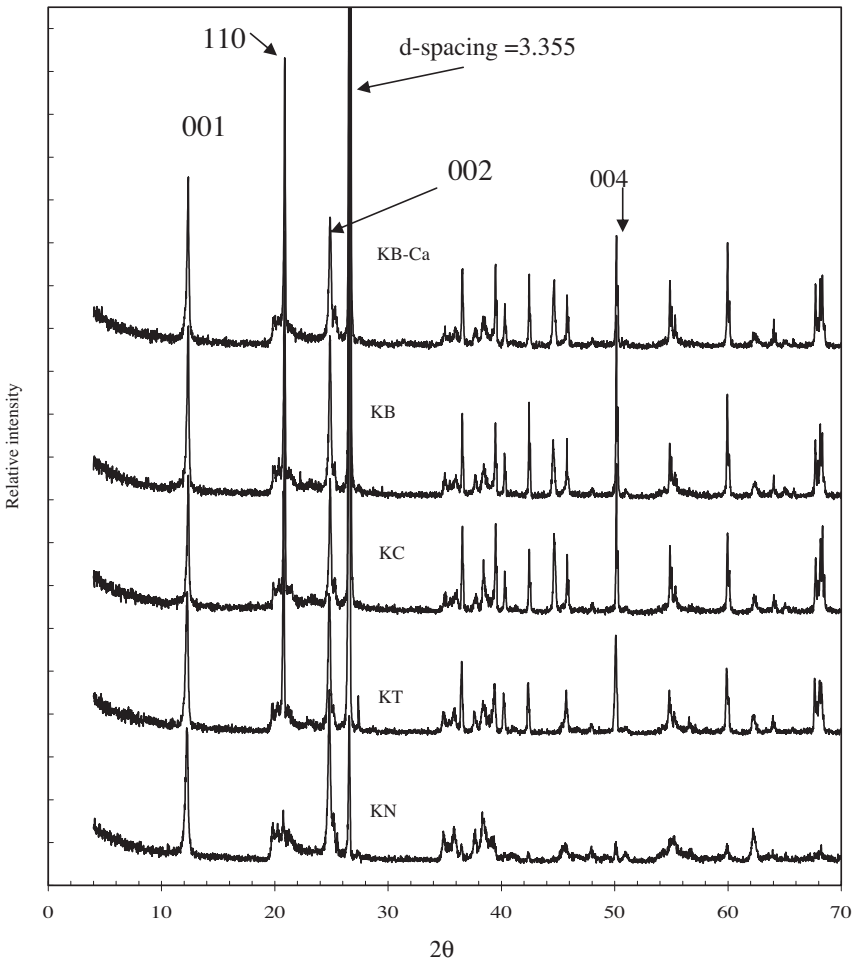

Figure 1 XRD patterns of different kaolinite samples.

prism planes such as 110 and basal planes such as 001, 002 and 004 are calculated for all modified samples. These I/I_o values for KT are 6.0, 1.1, 0.82 and 5.5 respectively, which indicated a sharp increase in the intensity of 110 and 004 peaks due to kaolinite treatment with H_2O_2, whereas I/I_o values slightly changed in other modified samples. These observations confirmed partial exfoliation/delamination which most probably resulted in particle size reduction [29]. The crystallite size (D) calculated using Scherrer's equation confirmed these results because D = 451.5 and 376.2 for KN and KT respectively. In addition, the peak at 2θ = 26.565° (d-spacing 3.355) becomes the most intense one confirming the isolation of silica as quartz [17–22,29]. The 004 reflection peak increased by calcination due to heat effect that caused an enlargement in kaolinite crystal size (D = 748.6) relative to KT (D = 376.2). The peak of the basal plane 001 in KN shifted to left and thus d-spacing of modified samples increased in the order KN (7.138) < KC (7.147) < KB (7.154) < KB-Ca (7.158) < KT (7.202). It is noticed that the decrease in crystal size for KT is accompanied by an increase in d-spacing or a decrease in the number of parallel plates per one kaolinite crystal relative to KN which may indicate partial exfoliation. Also, the d-spacing and the crystal size for KB-Ca (D = 1078.6) increased relative to KB (D = 748.2) due to ball milling with $CaSO_4$ mostly due to intercalation (pillaring) of $CaSO_4$ inside kaolinite layers [21].

3.1.2. FTIR- Spectroscopic analysis

FTIR of different samples is shown in Fig. 2. The bands at 3695 and 3653 cm^{-1} are assigned to Si–OH groups located either on the external surface or on internal point defects [30,31], and the band centered at 3615 cm^{-1} due to OH bridging Al and Si, with a strong Bronsted acidity. The absorption bands appeared in the region from 1088 to 400 cm^{-1} attributed to aluminosilicate structural frameworks, indicated that the chemical treatment with H_2O_2 resulted in some shift and the appearance of new overlapped bands with increasing intensity of the characteristic bands for terminal Si–OH, Al–OH and Si–O–Al in this region as shown in Fig. 2. These new overlapped bands disappeared after calcination in sample KC. These observations most probably resulted from separation of parallel plates in KT sample, followed by re-agglomeration of kaolinite particles due to heat effect in KC. Also, absorption bands of Si–O–Si and OH deformation, linked to Al^{3+} and Mg^{2+} at 843.2 cm^{-1} disappeared in KT sample whereas suffered a shift and/or splitting in other samples (KC, KB and KB-Ca) indicating some changes in the chemical environment, most probably due to parallel breakdown of parallel plates [32]. A small

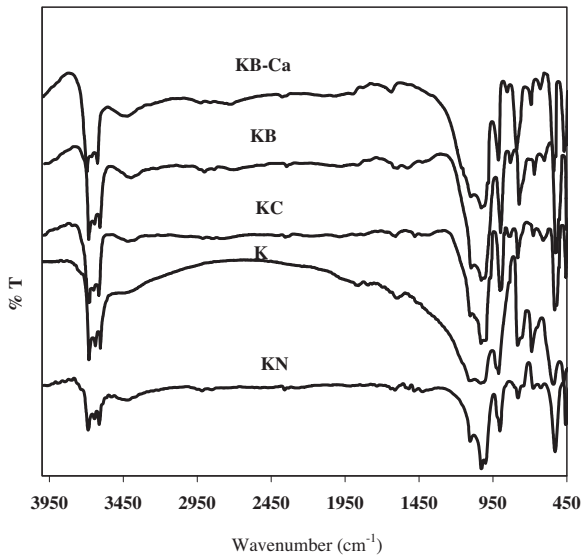

Figure 2 FTIR spectroscopic analysis of different kaolinite samples.

characteristic band of quartz appeared at 690.82 and 796.5 cm^{-1} in KN, their intensity increased in different modified samples as shown in Fig. 2 indicating the leaching of some metals from silica framework [19,22]. The absorbed water H-O-H stretching vibration band appeared in the range 3430–3412 cm^{-1} and bending vibration at around 1650 and 1622 cm^{-1} in all samples with a difference in their position and intensity [33]. Their intensity increased in the order: KT < KN < KC < KB < KB-Ca and also the intensity of AlOH deformation. This indicated that the surface hydroxyl groups of KC, KB and KB-Ca samples are increased, possibly due to forming more Si–OH and Al–OH groups [34,35]. However, the bending vibration of adsorbed water was observed in the same previous order, suggesting that the adsorbed water was increased due to water hydrogen bonding [21,31]. The presence of asymmetric stretching T–O (T = Si, M) can be observed more intense after ball milling at ~1240 and ~1080 cm^{-1}, due to more external and internal tetrahedral TO_4 vibrations, respectively. The spectra of all samples show additional features in the vicinity of the ~1085 and 805 cm^{-1} stretching bands, whose absorption frequency shifted upward after ball milling relative to pristine sample. These features can be assigned to more M–O–Si bending vibrations, indicating incorporation of hetero-atom into the clay-silica matrix [36]. The low frequency of the hydroxyl site in H- KB-Ca is explained in terms of a hydrogen-bonding perturbation of the corresponding proton by interaction with the framework oxygen atoms. The ~900 cm^{-1} band also is increased in intensity after ball milling and decreased after incorporation of $CaSO_4$. This result was explained by the 900 cm^{-1} band being essentially due to the increased degeneracy of the elongation vibration in the tetrahedral structure of SiO_4 induced by the change in the polarity of the M–O bonds when silicon is linked to another elements [37,38]. These results confirmed the exfoliation and delamination of kaolinite samples.

3.1.3. Scanning and transmission electron microscopy

SEM micrographs of KT and KC show nearly homogenous exfoliated/delaminated kaolinite platelets with particle size in the nano and micron ranges, Fig. 3. The KT sample shows low particle size caused by degradation or dissolution of lattice components in kaolinite minerals and the removal of organic materials that reduced agglomerating effect [39,40]. The KC sample is conglomerated into larger size particles due to heat effect. The images of ball milled KC sample with and without $CaSO_4$ (KB-Ca and KB, respectively) show more enlargement of particle size relative to KT. Fig. 4 shows HR-TEM (on the left) and their selective electron diffraction (SED) patterns (on the right) of KT, KB and KB-Ca samples. It was found that the plates of KT were well ordered as a single crystal after H_2O_2 treatment mostly due to exfoliation and elimination of some contaminants which resulted in smaller particles. HR-TEM and ring diffraction pattern of KB sample show that the sample is composed of multitude randomly-oriented crystals mostly due to separation of heteroatoms associated with defragments of quartz from silica as indicated by FTIR and XRD analysis. HR-TEM and spot diffraction pattern of KB-Ca sample indicated that kaolinite may be ordered as monocrystalline which interacted with other crystals of $CaSO_4$ through oxygen atom.

3.1.4. NH_3–TPD analysis

The amount of acid sites on the kaolinite surfaces was estimated by integration of the NH_3 desorption peaks and the results are shown in Table 1. The results showed that the acidity decreased due to chemical treatment in KT sample, unaffected by calcination, but increased due to ball milling with and without $CaSO_4$. The maximum temperature of weak and strong acid sites increased due to chemical and ball milling but decreased due to the effect of $CaSO_4$. Mostly, ball milling generated weak and strong acid sites but the weak is higher due to scission of Si–O–Al bond after ball-milling that increased

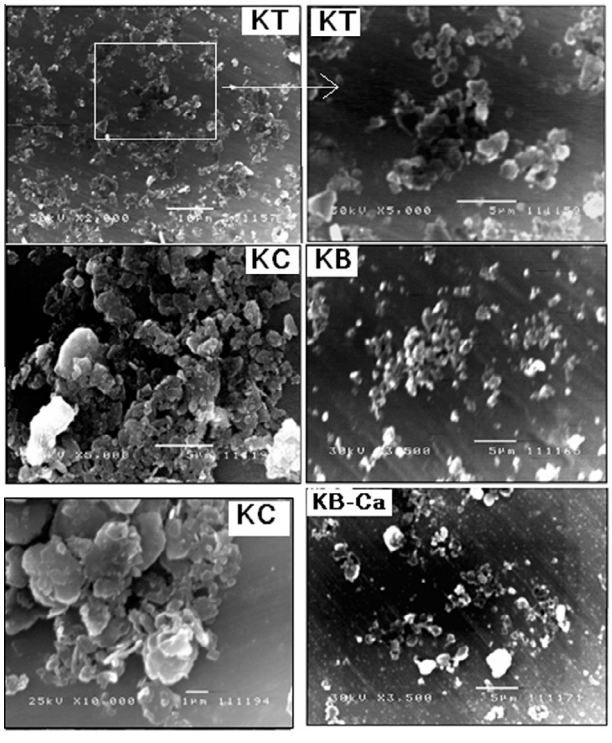

Figure 3 SEM micrographs of modified kaolinite samples.

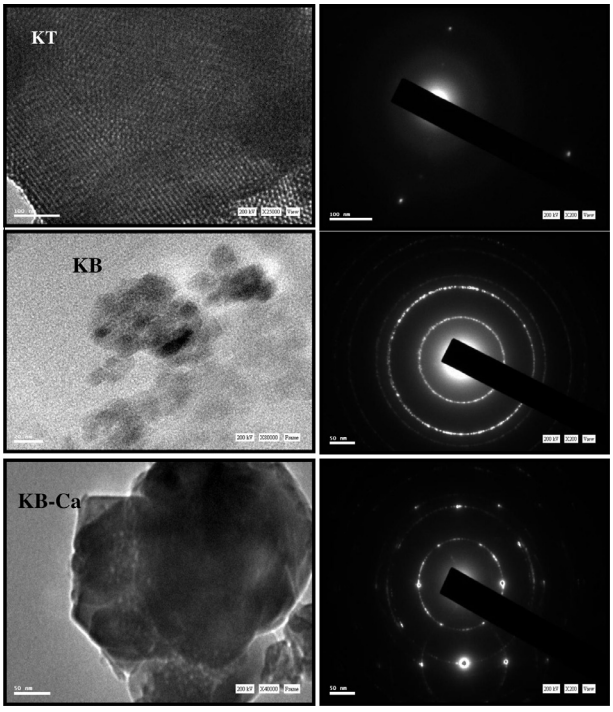

Figure 4 HR-TEM micrographs (on the right) and ring diffraction pattern (on the left) of KT, KB and KB-Ca samples.

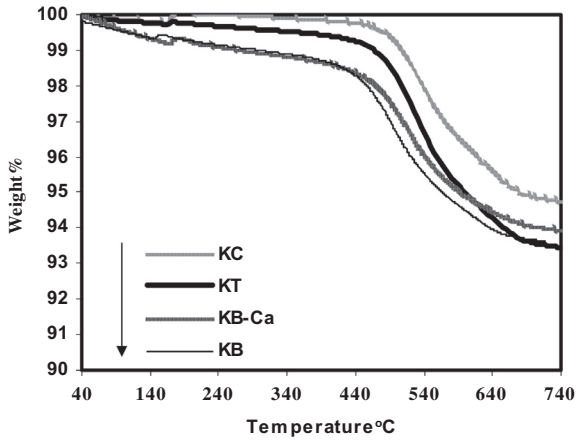

Figure 5 TGA thermograms of different catalyst samples.

silanol groups. The KB-Ca sample shows a higher proportion of strong and weak acid sites due to ball milling with the sulfate group that interacted with free silanol groups and alumina.

3.1.5. Thermogravimetric analysis (TGA) of different catalyst samples

TGA results of different catalyst samples (Fig. 5) indicated two steps of weight loss, from 50 to 455 °C and above 455 °C. The first weight loss increased with the order KC < KT < KB-Ca < KB and ranged from 0.3% to 3.0% as shown in the Figure. This is due to the libration of physisorbed water and water of crystallinity. This effect decreased in KC sample due to removal of organic materials and layer re-agglomeration during the thermal modification process. The second step in weight loss ranged from 5.5% to 3.5% with the same above-mentioned order. In this step, water is lost due to the thermal dehydroxylation process [21,26,41] or conversion of hydroxide compounds to oxide sample by desorption of water. The weight loss of KB is more than KB-Ca, which indicated grafting of the sulfate group on end capped and surface hydroxyl groups. The temperature of this second step started at 465.98 °C in KN as resulted in previous work [14]. In present samples, the dehydroxylation temperature shifted slightly to lower temperatures with the abovementioned order and related to breaking of hydrogen bonding between the adjacent kaolinite layers. This observation indicated structural crystal defects and coincided with the decrease in the particle size which resulted from delamination and exfoliation due to chemical and mechanical treatments confirmed by XRD, FTIR and SEM.

3.2. Methanol dehydration to dimethyl ether

Figs. 6–9 show the conversion percent (conv.%) of methanol dehydration and the yield percent (Y%) of DME produced using natural kaolinite (KN), chemically treated kaolinite (KT), ball milled kaolinite (KB) and ball milled kaolinite with $CaSO_4$ (KB-Ca) respectively at reaction temperature ranged from 200 to 500 °C and different contact times (15, 30 and 45 min).

Figs. 6 and 7 show the conv.% and the Y% of DME using natural kaolinite KN (studied in previous work) and KT respectively, at the same conditions for comparison [15]. Fig. 6 shows that the two curves of conv.% and the Y% at each contact time were identical only up to 300 °C which means complete selectivity to DME from 200 to 300 °C. As the reaction temperature increased, the conv.% and the Y% increased up to 450 °C but the selectivity to DME decreased to a large extent. So, the difference between the maximum

Table 1 Results of NH_3-TPD analysis of Parent kaolinite (KN), Treated kaolinite with H_2O_2 (KT), Calcined treated kaolinite (KC), Ball milled KC (KB) and Ball milled KC with $CaSO_4$ (KB-Ca).

Sample	Acidity (mmol NH_3/g cat.)			Max. temp. of weak	Max. temp. of strong	Max. Y% at 200 °C
	Weak	Strong	Total			
KN	0.011	0.005	0.016	162.3	511.4	10.3
KT	0.006	0.003	0.009	183.9	520.0	29.0
KC	0.006	0.003	0.009	165.0	518.7	—
KB	0.011	0.010	0.021	183.7	520.6	33.3
KB-Ca	0.013	0.082	0.095	179.2	493.9	30.8

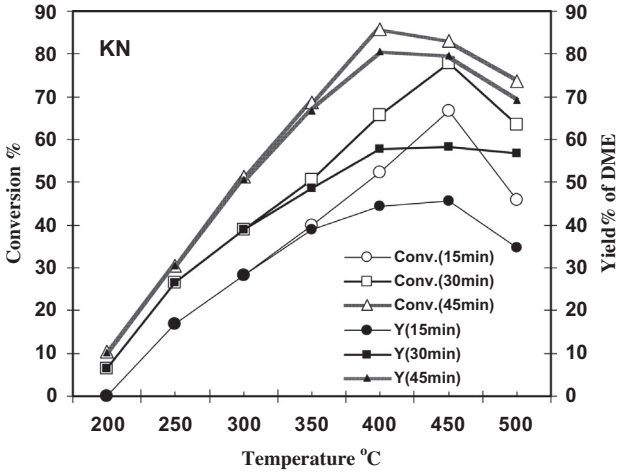

Figure 6 The effect of reaction temperatures on the conversion% of methanol (Conv.) and the yield% of DME (Y) at different contact times using KN sample.

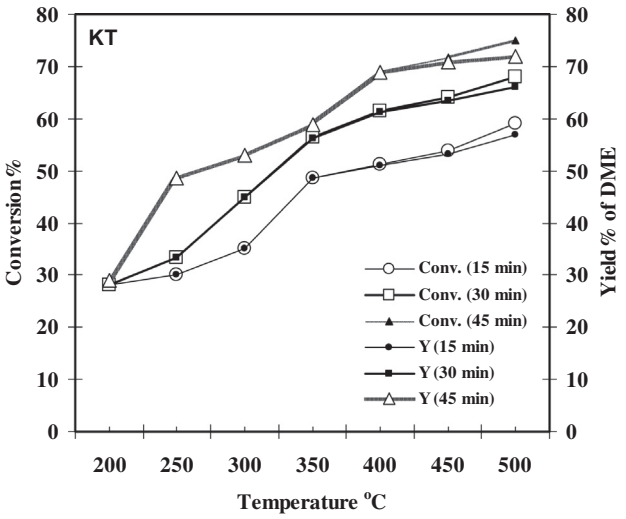

Figure 7 The effect of reaction temperatures on the conversion% of methanol (Conv.) and the yield% of DME (Y) at different contact times using KT sample.

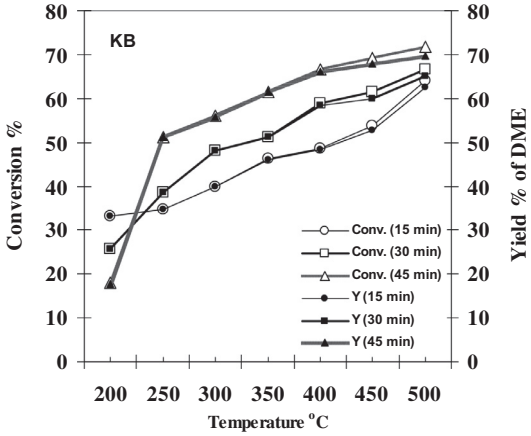

Figure 8 The effect of reaction temperatures on the conversion% of methanol (Conv.) and the yield% of DME (Y) at different contact times using KB sample.

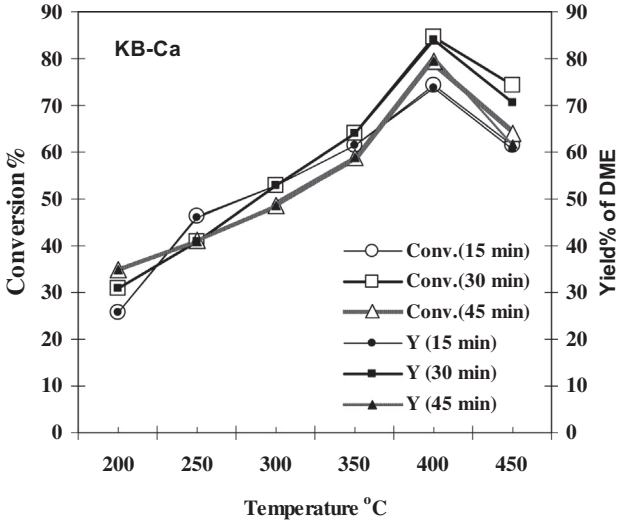

Figure 9 The effect of reaction temperatures on the conversion% of methanol (Conv.) and the yield% of DME (Y) at different contact times using KB-Ca sample.

conv.% and Y% was 5.2, 20.9 and 19.5 at 400 °C (45 min), 450 °C (15 and 30 min) respectively. The elevated reaction temperatures mostly activated the endothermic reaction (light olefin formation) which resulted in less selectivity to DME and coking which caused the catalyst deactivation. On the other hand, Fig. 7 shows that the conv.% and the Y% using KT sample increased with rising temperature up to 500 °C. Also, the two curves of conv.% and the Y% are identical up to 400 °C above which they are slightly separated with steady increase up to 500 °C. This means that KT has stable catalytic activity and better selectivity to DME up to 500 °C relative to KN. Also, KT sample have lower acidity relative to KN and thus lower activity at elevated temperatures but have higher activity at low temperatures (e.g. 200 °C) relative to their corresponding values at each reaction temperature using KN sample (see Table 1, Figs. 6 and 7). These results may be due to the creation of SiOH, AlOH and SiOHAl with higher strength and the elimination of some Bronsted and Lewis acid sites through a dehydration process or dissolution of some minerals [26,29]. The isolated silica (SiOH) may decrease the pore opening of some active sites and thus gave better selectivity to DME at all reaction conditions. Also the decrease in crystallite size and particle size in KT may result in a better accessibility of methanol molecules to the active sites, fast desorption of DME molecules at low reaction temperatures and less cocking at elevated reaction temperatures. So, the selectivity to DME increased and gave more stable catalytic activity above 400 °C. The maximum conv. % and Y% are 75 and 72 respectively after 45 min contact time and at 500 °C by using KT.

Fig. 8 shows the performance of KB sample in methanol dehydration. Its behavior is nearly the same as KT sample.

At lower temperatures, the conv. and thus the Y% increased sharply with rising temperature from 200 to 250 °C mostly due to higher acidity of KB sample relative to KT sample. Ball milling that resulted in a decrease in the thermal stability of KB sample (as shown in Fig. 5) most probably leads to a slight decrease in the catalytic activity relative to KT sample at high temperatures. The maximum conv.% and Y% are 72 and 70 respectively after 45 min contact time and at 500 °C by using KB.

Fig. 9 indicates the conv.% of methanol and the Y% of DME using ball milled kaolinite with $CaSO_4$ (KB-Ca). It is clear that ball milling of kaolinite with $CaSO_4$ improved the catalytic performance of KB-Ca sample mostly due to increased acidity. The conv.% and thus the Y% increased smoothly with rising temperature up to 400 °C with complete selectivity, then sharply decreased above this temperature mostly due to increasing amount of strong acidic sites which improved the side reactions and thus coking. The maximum conv. and Y% are 84.62 and 84 respectively at 400 °C and 30 min contact time. The maximum temperatures of acidic sites in KB-Ca decreased relative to KB which resulted in decreasing their strength and thus the catalytic activity of KB-Ca at low reaction temperatures but increased at high temperatures (up to 400 °C) as shown in table 1. The conv. and Y% start to decline at and above 400 °C, this may be due to the larger acidity relative to KT and KB samples which promotes the endothermic reactions producing olefins (so the selectivity decreased) which resulted in cocking and deactivation of KB-Ca.

3.3. The proposed reaction pathway

The mechanism of methanol dehydration reaction to DME has been discussed previously using aluminosilicates such as zeolites and bentonite [42,43]. It suggested two reaction routes to form dimethyl ether, via an alkoxonium cation intermediate and via alkoxy intermediate depending on the reaction conditions such as temperature and the acidic site strength. So, the pathway of methanol catalytic dehydration using modified kaolinite may proceed via the following two pathways: At low temperatures, the reaction proceeded via an Eley–Rideal type mechanism. In the transition state one methanol molecule forms a methoxonium ion, water leaves the molecule and simultaneously another weakly sorbed methanol binds to the methyl group forming protonated dimethyl ether. The protonated dimethyl ether donates immediately the proton back to the zeolite and desorbed (Eq. (1)). At elevated temperatures, a portion of the methanol molecules was transformed into methoxy groups (Eq. (2)). These methoxy groups react with weakly associated methanol to form dimethyl ether under simultaneous restitution of the hydroxyl group [14]. The reactivity of methoxy groups increases with the acid strength of the hydroxyl group it replaced [42]. Thus, the methoxy groups at weak OH produce dimethyl ether at lower temperatures than methoxy groups at strong OH. It is concluded that DME molecule needs two types of acidic sites, the first is more stronger than the second. So the selectivity to DME depends on the ratio between the strong and the weak + medium acid sites. When the amount of strong acid sites increased largely, the reaction yields side products such as olefins according to Eq. (3).

$$CH_3OH \xrightarrow{\text{OH-Cat}} CH_3OH_2^+ \xrightarrow[\text{OH-Cat.}]{CH_3OH} DME + H_2O + \text{HO-Cat.} \quad (1)$$

$$CH_3OH \xrightarrow[-H_2O]{\text{OH-Cat.}} CH_3O\text{-Cat.} \xrightarrow[\text{OH-Cat.}]{CH_3OH} DME + \text{HO-Cat.} \quad (2)$$

$$2CH_3OH + 2\text{HO-Cat.(strong)} \longrightarrow CH_2{=}CH_2 + 2H_2O \quad (3)$$

where HO-Cat. represents both SiOHAl and/or $SiOSO_3H$.

4. Conclusion

The chemical treatment of kaolinite with H_2O_2 resulted in partial exfoliation/ delamination of kaolinite, decreasing the amount of acidic sites by increasing their strength. Calcination has no effect on the acidity amount, decreased their strength and enlarged the particle size. Ball milling decreased the particle size, increased the amount of acidic sites with the same strength of KT sample resulted in increasing the catalytic activity at low temperature but decreased at high temperature. Calcination and ball milling create active Al–OH and Si–OH on the external surfaces (basal planes and edges) which interacted with $CaSO_4$ in KB-Ca. This interaction resulted in a creation of more acidic sites with slightly lower strength relative to KB. So the catalytic activity decreased at lower temperatures but increased at higher temperatures up to 400 °C then decreased with rising temperature. The catalytic activity increased by increasing the maximum temperature of acidic sites. The chemical and mechanical treatments resulted in complete selectivity to DME up to 400 °C and increased the thermal stability up to 500 °C except with $CaSO_4$ which gives the maximum selectivity to DME (84%) at 400 °C.

References

[1] S. Abello, D. Montane, Chem. Sus. Chem. 4 (2011) 1538–1556.
[2] S. Hassanpour, M. Taghizadeh, F. Ind, Eng. Chem. Res. 49 (2010) 4063–4069.
[3] I. Sezer, J. Therm. Sci. 50 (2011) 1594–1603.
[4] http://www.sciencedirect.com/science/article/pii/S1290072911000974[4] D-D. Liang, S-X. Liu, F-J. Ma, F. Wei, Y-G. Chen, Advan. Synth. & Catal. 353 (2011) 733–742.
[5] F. Zha, J. Ding, Y. Chang, J. Ding, J. Wang, J. Ma, Ind. Eng. Chem. Res. 51 (2012) 345–352.
[6] S.Y. Hosseini, M.R.K. Nikou, J. Am. Sci. 8 (2012) 218–225.
[7] S.Y. Hosseini, M.R.K. Nikou, J. Am. Sci. 8 (2012) 235–239.
[8] N. Hazari, E. Iglesia, J-A. Labinger, D-A Simonetti, Acc. Chem. Res. 45 (2012) 653–662.
[9] Y. Fu, T. Hong, J. Chen, A. Auroux, J. Shen, Surf. Thermochim. Acta 434 (2005) 22–26.
[10] N. Khandan, M. Kazemeini, M. Aghaziarati, Irani. J. Chem. Eng. 6 (2009) 3–11.
[11] D. Varisli, K.C. Tokay, A. Ciftci, T. Dogu, G. Dogu, Turk. J. Chem. 33 (2009) 355–366.
[12] J. Fei, Z. Hou, B. Zhu, H. Lou, X. Zheng, Appl. Catal. A 304 (2006) 49–54.
[13] J. Khom-in, P. Praserthdam, J. Panpranot, O. Mekasuwandumrong, Catal. Commun. 9 (2008) 1955–1958.
[14] S.M. Solyman, F.M. Tawfik, Egypt J. Pet. 19 (2010) 69–81.
[15] W.-H. Chen, B.-J. Lin, O.-M. Lee, M.-H. Huang, Appl. Energy 98 (2012) 92–101.

[16] R.D. Dragsdorf, H.E. Kissinger, A.T. Perkins, Soil Sci. Soc. Am. J. 71 (1951) 439–448.
[17] S. Milosevic, M. Tomasevic-Canovic, R. Dimitrijevic, M. Petrov, M. Djuricic, Am. Ceram. Soc. Bull. 71 (1992) 771–775.
[18] J.G. Miller, T.D. Oulton, Clays Clay Miner. 18 (1970) 313–323.
[19] Z. Juhasz, Acta Mineralogica-Petrographica 24 (1980) 121–145.
[20] R.L. Frost, E. Mako, J. Kristof, E. Horvath, J.T. Kloprogge, J. Coll. I. Sc. 239 (2001) 458–466.
[21] E. Makó, R.L. Frost, J. Kristof, E. Horváth, J. Coll. I. Sc. 244 (2001) 359–364.
[22] P.J. Sánchez-Soto, M.C. Jiménez de Haro, L.A. Pérez-Maqueda, I. Varona, J.L. Pérez-Rodríguez, J. Am. Ceram. Soc. 83 (2000) 1649–1657.
[23] R.L. Frost, J. Kristof, E. Horvath, J.T. Kloprogge, Langmuir 17 (2001) 3216–3222.
[24] E. Horváth, R.L. Frost, Eva Makóc, J. Kristóf, T. Cseh, Thermoch. Acta 404 (2003) 227–234.
[25] R. Schrader, Silikattechnik 21 (1970) 196–201.
[26] R.L. Frost, S.J. van der Gaast, Clay Miner. 32 (1997) 471–484.
[27] J.D.D. Melo, T.C. de Carvalho Costa, A.M. de Medeiros, C.A. Paskocimas, Ceram. Inter. 36 (2010) 33–38.
[28] R. Mikutta, M. Kleber, K. Kaiser, R. Jahn, Soil. Sci. Soc. Am. J. 69 (2005) 120–135.
[29] L.M. Laveulich, J.H. Wiens, Soli. Sci. Soc. Am. Proc. 34 (1970) 755–758.
[30] A. Zecchina, S. Bordiga, G. Spoto, L. Marchese, G. Petrini, G. Leonfanti, M. Padovan, J. Phys. Chem. B 96 (1992) 4991.
[31] A. Zecchina, S. Bordiga, G. Spoto, D. Scarano, G. Petrini, G. Leofanti, M. Padovan, C.O. Arean, J. Chem. Soc., Faraday Trans. 88 (1992) 2959–2969.
[32] W. Baikun, D. Hao, D. Yanxi, J. Wuhan Univ. Technol. – Mater. Sci. Ed. 25 (2010) 765–769.
[33] B.J. Saikia, G. Parthasarathy, J. Mod. Phys. 1 (2010) 206–210.
[34] X. Yan, L. Zhang, Y. Zhang, G. Yang, Z. Yan, Ind. Eng. Chem. Res. 50 (2011) 3220–3226.
[35] X.L. Ma, X.X. Wang, C.S. Song, J. Am. Chem. Soc. 131 (2009) 5777–5783.
[36] O.A. Anunziata, M.L. Martinez, M.B. Gomez Costa, Mater. Lett. 64 (2010) 545–548.
[37] D.A. Maria, L.H. Zhao, K. Jacek, J. Phys. Chem. 100 (1996) 2178–2182.
[38] B.L. Newalkar, J. Olanrewaju, S. Komarneni, Chem. Mater. 13 (2001) 552–557.
[39] J. Thorcl, Eur. Clay Groups 1985 (1983) 383–389.
[40] M. Drosdoff, E.F. Miles, Soil Sci. 46 (1938) 391–395.
[41] S. Letaief, J. Leclercq, Y. Liu, C. Detellier, Langmuir 27 (2011) 15248–15254.
[42] S.M. Solyman, M. Sadek, N.A.K. Aboul-Gheit, F.M. Tawfik, H.A. Ahmed, Egypt J. Pet. 22 (2013) 91–99.
[43] K. Hashimoto, Y. Hanada, Y. Minami, Y. Kera, Appl. Catal. A: Gen. 141 (1996) 57–69.